# Free-energy landscape of mono- and dinucleosomes: Enhanced rotational flexibility of interconnected nucleosomes

Gi-Moon Nam and Gaurav Arya*

*Department of NanoEngineering, University of California, San Diego, 9500 Gilman Drive, La Jolla, California 92093-0448, USA*

(Received 7 May 2015; revised manuscript received 10 February 2016; published 10 March 2016)

The nucleosome represents the basic unit of eukaryotic genome organization, and its conformational fluctuations play a crucial role in various cellular processes. Here we provide insights into the flipping transition of a nucleosome by computing its free-energy landscape as a function of the linking number and nucleosome orientation using the density-of-states Monte Carlo approach. To investigate how the energy landscape is affected by the presence of neighboring nucleosomes in a chromatin fiber, we also compute the free-energy landscape for a dinucleosome array. We find that the mononucleosome is bistable between conformations with negatively and positively crossed linkers while the conformation with open linkers appears as a transition state. The dinucleosome exhibits a markedly different energy landscape in which the conformation with open linkers populates not only the transition state but also the global minimum. This enhanced stability of the open state is attributed to increased rotational flexibility of nucleosomes arising from their mechanical coupling with neighboring nucleosomes. Our results provide a possible mechanism by which chromatin may enhance the accessibility of its DNA and facilitate the propagation and mitigation of DNA torsional stresses.

DOI: 10.1103/PhysRevE.93.032406

## I. INTRODUCTION

Eukaryotic DNA is organized into nucleosomes, each containing ∼146 base pairs (bp) of DNA wrapped around a histone octamer, separated by shorter stretches of naked DNA called linkers [1]. The array of nucleosomes folds into the chromatin fiber, which undergoes further coiling to yield chromosomes [2]. It is now well appreciated that chromosomes are highly dynamic entities, exhibiting a range of spontaneous and protein-mediated conformational changes that can be traced all the way down to individual nucleosomes [3–5]. In this study, we focus on one such functionally relevant conformational change, namely, the transition in the nucleosome linkers between negatively crossed, open, and positively crossed conformations, synonymous with the rigid-body rotation ("flipping") of nucleosomes about their linkers [6–9] [Fig. 1(c)].

In the canonical nucleosome, the two linker arms cross each other negatively, that is, with a negative linking number in topological terms [10]. However, rotation of the nucleosome about one of its linkers, in the direction opposite to that leading to steric clash between the two linker arms, causes the linkers to adopt an open conformation, and further rotation causes them to now cross each other positively. The ability of nucleosomes to flip between such states with distinct topologies allows for rapid exchange of torsional stresses between the DNA twist and writhe modes, thus providing a highly efficient mechanism for mitigating excessive torsional stresses in DNA [8,9,11]. We recently showed that nucleosome flipping also provides an efficient mechanism for propagating torsional stresses along the chromatin fiber and modulating its internal architecture [9,11]. Indeed, DNA twist propagation has been proposed as a plausible mechanism for gene regulation, where stresses generated at one site via processes like DNA transcription help melt twist-sensitive sequences at genomic locations distant from the stress origin [12,13]. Nucleosome flipping could also help modulate the accessibility of the linker DNA for protein invasion and binding [14], with open linkers arguably more accessible than crossed linkers, especially when they are roughly in plane with the nucleosome.

Nucleosome transitions across conformations with different linker crossings were first envisaged in experiments involving mononucleosomes assembled on short circular plasmids (DNA minicircles) [6,7]. The transitions were characterized in terms of a three-state model in which nucleosomes exhibit negative, open, or positive states corresponding to conformations with negatively crossed, open, and positively crossed linkers. Each state was assigned a linking number difference $\Delta$Lk, quantifying the extent of negative DNA supercoiling arising from both wrapped and linker DNA, and a free energy $\Delta G$, quantifying the thermodynamic stability, which were estimated by fitting the model to measurements of the overall linking number versus plasmid size. Other estimates for $\Delta$Lk and $\Delta G$ have been recovered from minicircles containing the 5S nucleosome positioning sequence [15] and from measurements of the twist-extension behavior of nucleosome arrays [8]. All estimates show that both the extent of negative supercoiling and the thermodynamic stability of the states decrease in the order negative > open > positive. While these measurements have provided useful information on the relative stabilities of the three nucleosomal states, a detailed, mechanistic understanding of the transition remains missing. It is also unclear how the relative stabilities of the three states are affected by the presence of other nucleosomes in an array, which are expected to introduce additional mechanisms for the mitigation of torsional stresses.

In this study, we sought a more detailed, fundamental understanding of the nucleosome flipping transition by computing the underlying free-energy landscape of a loosely end-tethered nucleosome along two reaction coordinates most relevant to the above transition: the linking number and the nucleosome tilt angle. The energy landscape was constructed from density-of-states Monte Carlo simulations of an established

*garya@ucsd.edu

 

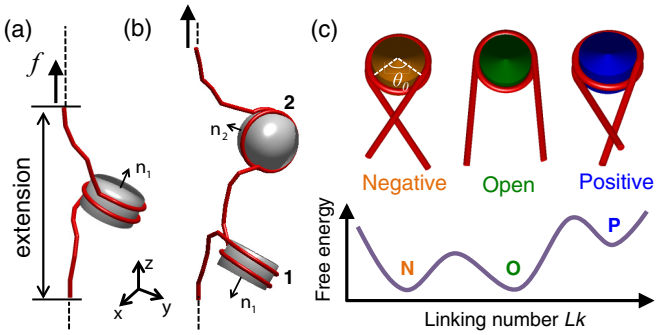


FIG. 1. Simulation setup used for studying the conformational transitions in (a) mononucleosomes and (b) dinucleosomes under a small tension $f$. The rotation of the nucleosome is measured by tracing its normal vector $\mathbf{n}$. (c) Schematic of the negative (orange), open (green), and positive (blue) nucleosomal states arranged along a schematic of the free-energy profile proposed in Ref. [11].

coarse-grained model of chromatin. To investigate the effect of neighboring nucleosomes, as would be present in a chromatin fiber, we also computed the energy landscape for a dinucleosome, the smallest representative of a nucleosome array that captures the mechanical coupling between nucleosomes while still being amenable to computations. The computed energy landscapes reveal key stable, metastable, and transition states associated with the flipping transition, and elucidate the array conformations and free energies corresponding to these states. The landscapes also reveal intriguing differences in the conformational fluctuations of mononucleosomes versus dinucleosomes that could have implications in chromatin structure, dynamics, and function.

## II. MODEL AND SIMULATIONS

The mononucleosome and dinucleosome are studied in a magnetic-tweezers-like setup [8,16], where one of the linker ends is held fixed, and the other end is subjected to an external force and is free to rotate and translate in the longitudinal direction [Figs. 1(a) and 1(b)]. Both systems are treated using a validated coarse-grained model of nucleosome arrays [9,11] in which the linker is modeled as a charged bead chain with a stretching, bending, and twisting modulus of DNA, and the nucleosome is treated as a charged rigid body. The relaxed length of the linkers is set to 21 nm, corresponding to ∼60 bp linkers observed in chicken erythrocyte chromatin [17]. The linker entry-exit angle is fixed to $\theta_0 = 120^\circ$, corresponding to ∼1.67 turns of wrapped DNA in nucleosomes [Fig. 1(c)]. All nonbonded components of the array interact via suitably parametrized screened electrostatic and excluded volume interactions. Throughout this study, we use a tension of 3.5 pN, a value typically used in single-molecule studies of nucleosomes, as this force is large enough to keep the array unfolded but still well below the critical force of nucleosome unraveling [18,19]. As in experiments, we study the systems at the physiological temperature of 300 K and a low monovalent salt concentration of 10 mM to avoid strongly attractive internucleosome interactions [17]. We refer readers to Refs. [9,11] for more details about this model.

Nucleosome conformations are characterized in terms of three states: negative, open, and positive, depending to how the entering and exiting linkers cross each other [Fig. 1(c)] [6]. Note that even though the fixed obtuse entry-exit angle predisposes the linkers to cross negatively, based on tangential extrapolation of linker paths from their nucleosome entry and exit points, this does not prevent the linkers from adopting open and positively crossed states depending on the forces and torques they experience. The three states are topologically distinct, each with a characteristic linking number Lk given by the sum of writhe Wr and twist Tw [7], with Lk ≈ −1.4, −0.7, and −0.4 for the negative, open, and positive states, respectively [8]. It is believed that the states are separated by energy barriers and transitions among them can be traced in Lk [see Fig. 1(c)].

To obtain the equilibrium conformational properties of the mononucleosome, we carry out Monte Carlo simulation using the density-of-states (DOS) method [20]. The main purpose of this method is to obtain the DOS $g(E)$ by sampling all possible conformational states at each energy level $E$. We further categorize these states into Lk and $\cos\theta$ to yield the joint DOS (JDOS) $g(E,\mathrm{Lk},\cos\theta)$, where $\cos\theta = \mathbf{n}\cdot\mathbf{z}$ ranges between −1 and +1. The angle $\theta$ measures the flipping of nucleosomes along the direction of tension that leads to changes in Lk and in the crossed state of the linkers (see snapshots $b$ and $g$ in Fig. 2). The computed JDOS $g(E,\mathrm{Lk},\cos\theta)$ then allows us to obtain the free-energy landscape

$$\beta F(\mathrm{Lk},\cos\theta) = -\ln\left[\sum_E g(E,\mathrm{Lk},\cos\theta)e^{-\beta E}\right], \qquad (1)$$

where $\beta \equiv 1/k_BT$ with Boltzmann constant $k_B$ and temperature $T$. The mean value of any thermodynamic quantity $A$ can then be obtained as a function of DNA topology via

$$\langle A(\mathrm{Lk})\rangle = \frac{\sum_{E,\cos\theta} A(E,\mathrm{Lk},\cos\theta)g(E,\mathrm{Lk},\cos\theta)e^{-\beta E}}{\sum_{E,\mathrm{Lk},\cos\theta} g(E,\mathrm{Lk},\cos\theta)e^{-\beta E}}. \qquad (2)$$

Calculating 3D JDOSs is much more computationally demanding than calculating DOSs. Thus, we use the global update method for more efficient sampling [20,21]. The final result of the JDOS is refined by averaging over 20 independent runs.

Evaluating the JDOS of a dinucleosome in a manner similar to the mononucleosome, involving simultaneous tracing of the linking number and orientation of *each* nucleosome, is computationally challenging. To this end, we compute the JDOS as a function of the *overall* linking number Lk and of the correlation $C_{\mathrm{nuc}} \equiv \mathbf{n}_1\cdot\mathbf{n}_2$ between the two nucleosomes, where $\mathbf{n}_1$ and $\mathbf{n}_2$ are the normal vectors of the two nucleosome [see Fig. 1(b)]. Similar to $\cos\theta$ for mononucleosomes, $C_{\mathrm{nuc}}$ also ranges between −1 and +1 corresponding to "out-of-phase" and "in-phase" nucleosomes, respectively. We then obtain the free energy $\beta F(\mathrm{Lk},C_{\mathrm{nuc}})$ and ensemble averages in thermodynamic quantities $\langle A(\mathrm{Lk})\rangle$ from the computed JDOS using expressions similar to Eqs. (1) and (2), in which $\cos\theta$ has been replaced by $C_{\mathrm{nuc}}$.

The Appendix provides more details on the implementation of the DOS method for the mononucleosome and dinucleosome systems.

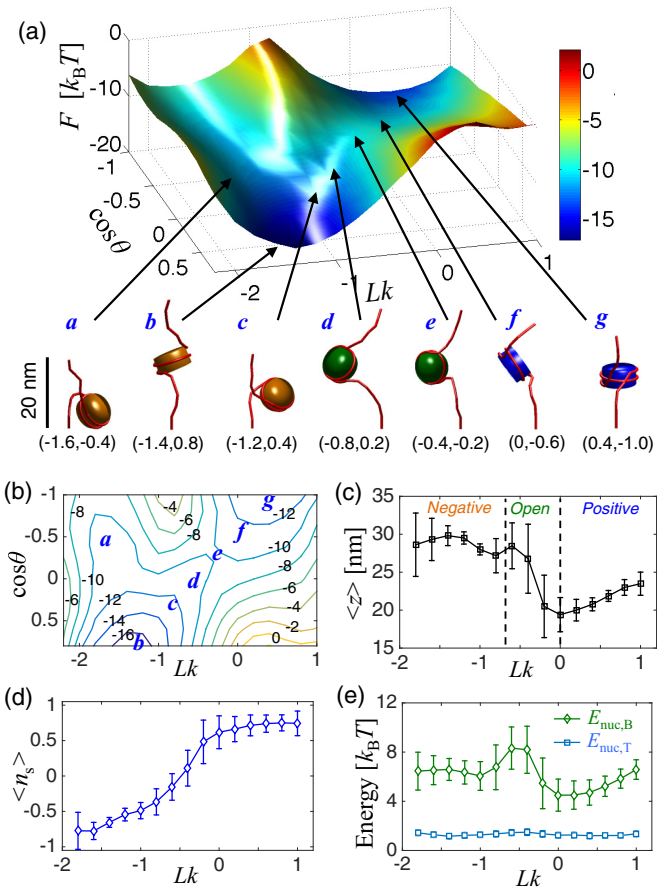


FIG. 2. (a) Free-energy landscape of a mononucleosome subjected to 3.5 pN tension as a function of Lk and $\cos\theta$. Also shown are representative conformations sampled from the simulations at different portions of the landscape indicated by the (Lk, $\cos\theta$) value. (b) Contour plot of free-energy landscape with free-energy values labeled in units of $k_BT$. (c) Mean extension $\langle z\rangle$, (d) nucleosomal state $\langle n_s\rangle$, and (e) linker bending and twisting energy as functions of Lk. In all panels, the error bars indicate the corresponding fluctuations. The dashed lines in (c) represent approximate boundaries between negative, open, and positive states in Lk.

## III. RESULTS

Figure 2(a) shows the computed free-energy landscape of the mononucleosome as a function of Lk and $\cos\theta$ along with representative nucleosome conformations at various points along the landscape. We observe bistability in nucleosomal states with the global and local minima located at (Lk, $\cos\theta$) $\approx$ $(-1.4,0.8)$ and $(0.4,-1.0)$, respectively. The global minimum (labeled $b$ in the figure) indicates a stable state and corresponds to a nucleosome with negatively crossed linkers (see the conformation labeled $b$), while the local minimum (labeled $g$) indicates a metastable state and corresponds to a nucleosome with positively crossed linkers (conformation $g$). The two states exhibit a free-energy difference of roughly $4k_BT$ and are separated by an energy barrier at roughly $(-0.4,-0.2)$. This transition state (labeled $e$) corresponds to a nucleosome with open linkers (conformation $e$). The energy barrier from the negative state ($\approx 6k_BT$) is noticeably higher than the barrier from the positive state ($\approx 2k_BT$). The contour map in Fig. 2(b) shows a straight minimum-free-energy transition pathway between the negative state $b$ and the positive state $g$ via the open state $e$, suggesting that this transition occurs by nucleosome flipping, which is characteristically accompanied by changes in both Lk and $\theta$.

The higher stability of the negative state may be attributed to the greater rotational freedom that the nucleosome possesses in this state as compared to the positive state, where the linkers experience significant steric and electrostatic repulsion when the nucleosome is rotated further in the +Lk direction. In contrast, the negative state allows further rotation of the nucleosome towards a negatively overwound state located at approximately $(-1.6, -0.5)$ (labeled $a$). Note that this transition takes place with a minimal change in Lk, reflecting interconversion between Tw and Wr twisting modes.

The variation of the mean nucleosomal state $\langle n_s\rangle$ with Lk is plotted in Fig. 2(d), where the state variable $n_s$ is assigned a value of $-1$, 0, and $+1$ for negative, open, and positive states, respectively. The results confirm the prevalence of negative and positive nucleosomes at Lk values corresponding to the stable and metastable states in the energy landscape, and that of open nucleosomes at intermediate Lk values corresponding to the transition state. In particular, the range $-0.8 \lesssim \mathrm{Lk} \lesssim 0$ corresponds to the transient formation of the open state. As the nucleosome adopts this state, its extension decreases rapidly from approximately 30 to 20 nm and begins to display large fluctuations [Fig. 2(c)]. These fluctuations are related to the instability in the orientation of the nucleosome along the $+z$ axis (see conformation $e$), likely due to torques imposed on the nucleosome by strongly bent linkers. We therefore measured the Lk dependence of the mean bending and twisting energy of the entry and exit linker segments attached to the nucleosome (not the entire linkers), denoted by $\langle E_{\mathrm{nuc},B}\rangle$ and $\langle E_{\mathrm{nuc},T}\rangle$ and plotted in Fig. 2(e). As expected, $\langle E_{\mathrm{nuc},T}\rangle$ remains stationary over the entire range of Lk, due to rapid adjustment of the nucleosome orientation in response to changing Lk, while $\langle E_{\mathrm{nuc},B}\rangle$ becomes large in the Lk range corresponding to the open state. This large bending energy is also most likely responsible for the energy barrier at the open state.

The bistability observed in mononucleosome simulations is in sharp contrast to the stable open state observed in nucleosomes reconstituted on small circular plasmid DNA [6,7] as well as to Brownian dynamics simulations of nucleosome arrays using the same coarse-grained model as employed here [11]. In these experiments, the open conformation of the linkers is stabilized by the tension they experience from the rest of the plasmid which forms a highly strained loop. This suggests that equilibrium between the nucleosomal states could be altered in arrays where nucleosomes exert similar tensile forces on neighboring nucleosomes. To examine how the conformational fluctuations of a nucleosome are affected by the presence of neighboring nucleosomes, we considered dinucleosomes in the same simulation setup as the mononucleosome studied above. The dinucleosome system allows us to investigate the effects of mutual mechanical interplay between adjacent nucleosomes with negligible effect from array supercoiling and stacking interactions between next-neighbor nucleosomes. As explained before, the free-energy landscape of the dinucleosome is computed as a function of the overall

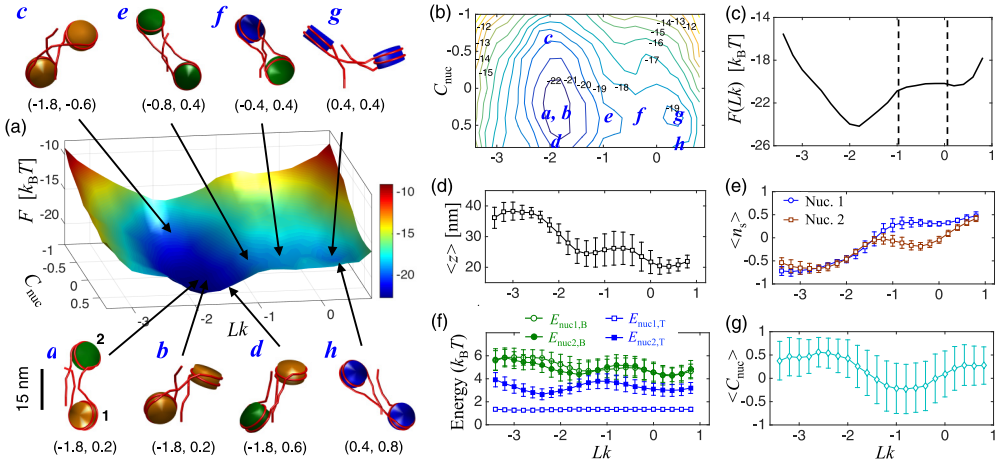


FIG. 3. (a) Free-energy landscape of the dinucleosome subjected to 3.5 pN tension as a function of Lk and $C_{\text{nuc}}$, along with representative conformations at different portions of the landscape. (b) Contour plot of the free energy with indicated free-energy values in units of $k_BT$, showing a possible transition pathway via region $e$. (c) Plot of a one-dimensional free-energy profile as a function of Lk. Mean values of the (d) extension $\langle z \rangle$, (e) nucleosomal states $\langle n_s \rangle$, (f) local linker bending and twisting energy, and (g) nucleosome correlation $C_{\text{nuc}}$ plotted as functions of Lk. The dashed lines in (c) represent edges of the plateau region.

linking number Lk and the correlation $C_{\text{nuc}}$ between the two nucleosomes.

The resulting free-energy landscape of the dinucleosome and its representative conformations at select points across the landscape are shown in Fig. 3(a). The landscape has a global minimum located at $(\text{Lk}, C_{\text{nuc}}) \approx (-1.8, 0.2)$ (labeled $a$ in the figure) and is more stretched along the $C_{\text{nuc}}$ axis [Fig. 3(b)]. Nucleosomes exhibit a mixture of in-phase negative and open states within this minimum, where all three possible combinations of nucleosome states are observed, i.e., both negative, both open, and one negative, one open [conformations labeled $a$–$d$; Fig. 3(e)]. The energy landscape also has a shallow, local minimum at approximately (0.4,0.4) (labeled $g$), where both nucleosomes adopt in-phase, positive states (conformations $g$ and $h$). The two minima exhibit a free-energy difference of roughly $3k_BT$ and are separated by an energy barrier of roughly $4k_BT$ from the global minimum. The barrier is located at $C_{\text{nuc}} \approx 0.4$ and spread over a broad range of Lk values spanning $-1.5 < \text{Lk} < 0$ (labeled $e$ and $f$). This barrier appears as a plateau along Lk in the $C_{\text{nuc}}$-averaged free-energy profile in Fig. 3(c). On this plateau, the dinucleosome consist of a mixture of open and positive states [conformations $e$ and $f$; Fig. 3(e)].

The presence of multiple nucleosomal states across most portions of the energy landscape and its broadening along Lk are direct consequences of the increased rotational freedom of nucleosomes when present in an array. In other words, mechanical stresses generated by the rotation of one nucleosome are easily accommodated by the rotation of the neighboring nucleosome with minimal changes in free energy. This effect may be gleaned from the Lk dependence of the mean bending and twisting energy of linker segments attached to the nucleosome [Fig. 3(f)], which appear to be anticorrelated, implying mutual constraint between the two modes. The increased rotational flexibility of nucleosomes helps lower the free-energy barrier of transition between the stable and metastable states, from roughly $6k_BT$ and $2k_BT$ for the forward and reverse transitions in mononucleosomes to roughly $4k_BT$ and $1k_BT$ in dinucleosomes [Fig. 3(c)]. Thus, the nucleosomes in an array are readily driven out of phase [Fig. 3(g)] into longer-lived open states as compared to nucleosomes in isolation, where the open state appears much more infrequently.

Further analysis reveals that the average extension $\langle z \rangle$ of the dinucleosome decreases in a steplike manner with increasing Lk [Fig. 3(d)]. This behavior is a manifestation of the sequential flipping of nucleosomes from negative to open to positive conformations, which require progressively decreasing end-to-end extensions to minimize their free energy. The extension profile has a striking resemblance to the entry and exit linker segment bending energy profile $\langle E_{\text{nuc},T} \rangle$ [Fig. 3(f)], indicating that the extension of linkers away from the dinucleosome plane requires them to bend sharply at their nucleosomal entry or exit site.

## IV. DISCUSSION

The computed energy landscapes reveal important differences in the flipping transition of isolated nucleosomes versus those present in a dinucleosome: Isolated nucleosomes exhibit stable negative and positive states, and the open state appears only as a short-lived transition state; in contrast, the open state is stabilized and appears frequently in the dinucleosome. Assuming that the linker DNA is more accessible for protein binding in open than crossed conformations, especially when the linkers are roughly in plane with the nucleosome, then the linker DNA should be more accessible in dinucleosomes as compared to an isolated nucleosome [22]. This conjecture is supported by studies examining differences in the restriction-enzyme digestion pattern of DNA templates folded into single nucleosomes versus dinucleosomes, where it was found that restriction sites are nearly eight times more accessibile in loosely folded dinucleosomes as compared to mononucleosomes [14]. Recent single-molecule Förster resonance energy transfer (FRET) measurements [23] show that linkers exhibit more open conformations when connected

to neighboring nucleosomes, consistent with our findings. The formation of open nucleosomes may act as a precursor to the access of proteins to nucleosomal DNA. Once an initial entry has been made, the energy barrier to the open state should become sufficiently low to accommodate additional proteins, consistent with the concept of cooperative binding of proteins to DNA target sites [24]. Thus, the increased prevalence of open nucleosomes in dinucleosomes, and conceivably in longer arrays, could enhance not only the accessibility of linker DNA but also conceivably that of nucleosomal DNA.

The increased stability of the open state in dinucleosomes originates from the ability of neighboring nucleosomes to absorb residual mechanical stresses, from the open nucleosome, by adopting negative or positive states. This causes significant lowering of the free-energy barrier separating the negative and positive states, leading to more rotationally flexible nucleosomes. Extending to arrays, this effect could contribute to the high torsional resilience of chromatin, whereby it can accommodate a large amount of external twisting before undergoing global supercoiling, as observed in both experiments and simulations [8,11,25]. The enhanced rotational flexibility of nucleosomes in arrays would then also be expected to facilitate the propagation of DNA twist along the nucleosome array, which requires nucleosome flipping motions to transmit the twist from one linker to the next [9]. Interestingly, the dinucleosome adopts a "twisted paperclip" structure at the free-energy minimum [conformation *b* in Fig. 3(a)] with slightly diverging end linkers and nearly orthogonal nucleosomes, reminiscent of the repeating dinucleosome motif in the crystal structure of a tetranucleosome [26]. This similarity suggests that the arrangement of nucleosomes in tetranucleosomes might not be solely determined by internucleosome interactions and packing constraints, but that mechanical coupling between nucleosomes via their linkers, as demonstrated here, could also play some role.

The energy landscapes presented here were obtained for specific values of applied tension, salt concentration, and linker length. We anticipate that increasing the applied force should increasingly tilt the energy landscape towards those conformations that exhibit large end-to-end extensions [27]. Thus, we expect the open state that has the potential to contribute the largest length of DNA to this extension, albeit at the cost of strongly bent linkers, to become increasingly stabilized with increasing tension. Increasing the monovalent salt concentration, beyond the 0.01 M used here, should alleviate the electrostatic repulsion between the linkers [28] and help further stabilize the crossed configurations of the linkers. The effect of linker length is likely opposite, with increasing length leading to an increase in the electrostatic repulsion between the linkers, causing some destabilization of the crossed states relative to the open state. Additional studies are required to test these speculations.

As a final note, we would like to emphasize that our nucleosome model does not account for "breathing" dynamics [24,29–31], a phenomenon where the nucleosomal DNA can spontaneously unwrap from its ends to allow brief access to DNA sites before rewrapping. It is difficult to predict the impact of such fluctuations on the computed energy landscape. One would expect the effect to be minimal at small forces, given that the fluctuations occur spontaneously and are therefore associated with free-energy changes of $\sim k_B T$. However, at forces larger than 2–3 pN [19,32], the outer turn of nucleosomal DNA is expected to unwrap from the surface of the octamer, the physics of which has already been elucidated [33,34]. This could potentially lead to a new stable state with widely open linkers that cannot be characterized using the computed energy landscape; an additional reaction coordinate accounting for the extent of DNA unwrapped from the octamer would be required. Such unwrapping of DNA, which could also be triggered by external torques [35], might provide an additional mechanism for the relaxation of torsional stresses in chromatin, and it would be interesting to examine how such a mechanism would compare against the nucleosome flipping mechanism investigated here. Under extreme circumstances of positive supercoiling, e.g., during transcription, the DNA may even completely unwrap from the octamer and rewrap with the opposite chirality to relieve such excessive stresses [36].

## V. CONCLUSION

We have computed the free-energy landscape of a mononucleosome and of a dinucleosome to investigate differences between the flipping transition of nucleosomes in isolation and those present in an array, and thereby affected by neighboring nucleosomes in the array. The energy landscapes reveal that individual nucleosomal transitions between stable states with negatively and positively crossed linkers can be made at much lower free-energy cost in dinucleosomes as compared to isolated nucleosomes. In particular, the intermediate conformation with open linkers that appears as a high-energy transition state in mononucleosomes now becomes part of the stable state in dinucleosomes. This increased stability of the open state is shown to arise from the ability of the neighboring nucleosome to accommodate residual torsional stresses of the open nucleosome by flipping into negative or positive states. This unique mechanism leads to rotationally flexible nucleosomes with more open linkers, on average, which may have important implications in chromatin function, namely, in increasing the accessibility of linker and nucleosomal DNA, enhancing the torsional resilience of chromatin fibers, and facilitating the propagation of DNA twist. While we focused on the interplay between nucleosomes in a dinnucleosome, this prototypical system is expected to capture the essence of the mechanical coupling between nucleosomes, and the effects predicted here should be applicable, if not magnified, in longer nucleosome arrays.

## ACKNOWLEDGMENTS

We thank the American Chemical Society Petroleum Research Fund (Award No. 52515-ND7) for partial support. The computational calculations were carried out at PLSI supercomputing resources of the Korea Institute of Science and Technology Information.

## APPENDIX

The aim of this work is to compute the joint density of states (JDOS) in three variables $g(E,\mathrm{Lk},C)$ where $E$ is the total energy, Lk is the total linking number, and $C$ is an

additional variable that characterizes nucleosome orientation. In the case of a mononucleosome, $C = \cos\theta$ characterizes the orientation of the nucleosome relative to the direction of tension, and in nucleosome arrays, $C = C_{\rm nuc}$ characterizes the relative orientation or correlation between adjacent nucleosomes. Once $g(E,\mathrm{Lk},C)$ is known, the partition function can be calculated as

$$Z(T) = \sum_{E,\mathrm{Lk},C} g(E,\mathrm{Lk},C)\exp(-E/k_BT), \qquad \text{(A1)}$$

and important thermodynamic quantities such as the free energy, end-to-end distance, and nucleosomal state can be calculated as functions of temperature $T$ and one or both of the order parameters Lk and $C$.

To compute $g(E,\mathrm{Lk},C)$, we use the Wang-Landau Monte Carlo (MC) sampling approach in which conformational states are sampled with a probability proportional to the inverse of the JDOS so as to achieve uniform sampling of each energy level in the system [20]. At the beginning, the JDOS is unknown and the MC simulations are started with an initial guess of the JDOS. The JDOS is then updated at each MC step until one obtains a flat histogram of energy levels visited during the simulation and the JDOS has converged to its true value. However, it is very computationally demanding to sample a three-dimensional JDOS, compared to the usual one-dimensional DOS $g(E)$. Moreover, thermodynamic systems generally have a very small DOS approaching their ground state, which is the most critical issue hampering uniform sampling over all energy levels.

To overcome these difficulties, we have implemented recent enhancements proposed by Zhou *et al.* [20] that involve local and global updates of the JDOS. The local update is carried out by using a kernel function. The main purpose of this function is to update $g(E,\mathrm{Lk},C)$ for the selected state as well as its neighboring states. This is especially useful for continuous models, which involve a large number of conformational states. As in the original article, we implemented a Gaussian kernel function $k(x) = \exp(-x^2/\delta^2)$, where $x$ denotes a particular state $(E,\mathrm{Lk},C)$ collectively, and the width $\delta$ is set to 0.1 in our simulation. Note that in practice we calculate the logarithmic value of $g(x)$ as $w(x) = \log_\alpha g(x)$, in order to prevent numerical divergence in $g(x)$, where $\alpha$ is a rescaling factor for $w(x)$. The global update (see below) is carried out to promote sampling of important but unexplored regions of the phase space.

Below, we summarize the essential steps of our implementation of this method and provide relevant parameters corresponding to each step.

(1) Prior to the simulation, we specified the range of each variable of interest to sample with an appropriate bin size, as given by

$$\begin{aligned} -15 &\leqslant E/k_BT \leqslant 450, \quad \Delta E = 5, \\ -2.0 &\leqslant \quad \mathrm{Lk} \quad \leqslant 1.0, \quad \Delta\mathrm{Lk} = 0.2, \\ -1.0 &\leqslant \quad C \quad \leqslant 1.0, \quad \Delta C = 0.2. \end{aligned} \qquad \text{(A2)}$$

The simulations were started with an initial setting of $w(x) = 0$ over the entire 3D macroscopic phase space $x$.

(2) By performing a random walk within the phase space, $w(x)$ is locally updated by the Gaussian kernel function as follows:

$$w(x) \to w(x) + \gamma k[(x - x_0)/\delta], \qquad \text{(A3)}$$

where $x_0$ indicates a trial state arrived at by a random walk within the phase space; $\gamma$ and $\delta$ are the magnitude and width of the kernel, which are chosen as 0.01 and 0.2, respectively. Note that $\gamma$ is chosen to be comparable to the assigned bin size.

(3) A trial state $x_{\rm new}$, from the current state $x_{\rm old}$, is accepted with a probability

$$P(x_{\rm old} \to x_{\rm new}) = \min[1, \exp(-\Delta w \ln\alpha)], \qquad \text{(A4)}$$

where $\Delta w = w(x_{\rm new}) - w(x_{\rm old})$. The $\ln\alpha$ term is introduced into the acceptance criterion to make $w(x)$ converge to $\log_\alpha g(x)$. The choice of $\alpha > 1$ does not change the final estimation of $w(x)$, but rather determines the acceptance rate by rescaling $w(x)$. In our simulations, we chose $\alpha = 2$, which leads to a minimal rescaling in $w(x)$, but yields a higher probability for a low-energy state to be accepted.

(4) To enhance the sampling of low-energy regions, we applied the following global update to $w_T(x)$; the $w(x)$ accumulated until a specified intermittent point $T$ during the MC simulation:

$$\begin{aligned} w_T(x) \to\ & w_T(x) \\ & + \kappa \exp\left[\frac{-\lambda}{w_T(x) - \omega}\right]\Theta(w_T(x) - \omega), \end{aligned} \qquad \text{(A5)}$$

where $w_T(x)$ is shifted up by an amount of $\kappa$, only for the regions where $w_T(x) > \omega$. We chose $\kappa = 2.0$ and $\omega = 0.5$. $\Theta$ is the Heaviside step function, given by 0 and 1 for $w_T(x) < \omega$ and $w_T(x) > \omega$, respectively. This global update gives rise to a discontinuity in $w(x)$ between the frequently and rarely visited regions, resulting in better sampling of the unexplored regions. Note that $\lambda$ determines a decay rate for the discontinuous regions, and we chose $\lambda = 0.2$.

(5) We continue the MC simulation, implementing only the local update (steps 2 and 3) until a uniform growth in $w(x)$ at the boundary of the elevated regions is observed. If uniform growth is declared, a global update is applied (step 4). The simulation finishes when $w(x)$ expands to the entire area of interest.

For statistical accuracy, the JDOS can be refined either by applying a strict criterion on declaring uniform growth or by taking averages over multiple independent runs. Generally, the former demands a higher computational effort to satisfy the criterion. In our simulation, the JDOS was refined with 20 independent runs.

We implemented two types of MC moves for sampling the conformations of the nucleosome complex: translational and twist moves [21]. The translational move was carried out via a random displacement of a randomly chosen linker bead or nucleosome core. To ensure high acceptance probability, the magnitude of random displacement is restricted to a value smaller than the equilibrium bond length $l_0 = 3$ nm between linker beads. A pure twist move involved rotating a randomly chosen linker bead by a random angle, picked from a uniform distribution within $\pm\pi$ about the bond vector pointing toward the next bead [11]. In addition to these local moves, we also implemented a global pivot move. This move was introduced to allow better sampling of nucleosome orientations, which

are key to the nucleosomal state transitions studied here. In this move, a randomly chosen nucleosome core is rotated by a random angle about an axis defined by two beads on two opposite linkers. In our sampling scheme, this move plays an important role in preventing the nucleosome from being trapped at a local energy minimum.


[1] T. J. Richmond and C. A. Davey, Nature (London) **423**, 145 (2003).

[2] G. Felsenfeld and M. Groudine, Nature (London) **421**, 448 (2003).

[3] C. L. Woodcock and R. P. Ghosh, Cold Spring Harbor Perspect. Biol. **2**, a000596 (2010).

[4] K. Luger, Chromosome Res. **14**, 5 (2006).

[5] J. C. Hansen, Annu. Rev. Biophys. Biomol. Struct. **31**, 361 (2002).

[6] A. Prunell and A. Sivolob, in *Chromatin Structure and Dynamics: State-of-the-Art*, edited by J. Zlatanova and S. H. Leuba (Elsevier, London, 2004), Vol. 39, p. 45.

[7] F. De Lucia, M. Alilat, A. Sivolob, and A. Prunell, J. Mol. Biol. **285**, 1101 (1999); **295**, 55 (2000).

[8] A. Bancaud, N. C. e Silva, M. Barbi, G. Wagner, J.-F. Allemand, J. Mozziconacci, C. Lavelle, V. Croquette, J.-M. Victor, A. Prunell, and J.-L. Viovy, Nat. Struct. Mol. Biol. **13**, 444 (2006).

[9] I. V. Dobrovolskaia, M. Kenward, and G. Arya, Biophys. J. **99**, 3355 (2010).

[10] A. D. Bates and A. Maxwell, *DNA Topology* (Oxford University Press, New York, 2005).

[11] G.-M. Nam and G. Arya, Nucleic Acids Res. **42**, 9691 (2014).

[12] C. Lavelle, Nat. Struct. Mol. Biol. **15**, 123 (2008).

[13] F. Kouzine, S. Sanford, Z. Elisha-Feil, and D. Levens, Nat. Struct. Mol. Biol. **15**, 146 (2008).

[14] M. G. Poirier, M. Bussiek, J. Langowski, and J. Widom, J. Mol. Biol. **379**, 772 (2008).

[15] A. Sivolob, C. Lavelle, and A. Prunell, J. Mol. Biol. **326**, 49 (2003).

[16] R. Vlijm, M. Lee, J. Lipfert, A. Lusser, C. Dekker, and N. H. Dekker, Cell Rep. **10**, 216 (2015).

[17] S. A. Grigoryev, G. Arya, S. Correll, C. Woodcock, and T. Schlick, Proc. Natl. Acad. Sci. USA **106**, 13317 (2009).

[18] B. D. Brower-Toland, C. L. Smith, R. C. Yeh, J. T. Lis, C. L. Peterson, and M. D. Wang, Proc. Natl. Acad. Sci. USA **99**, 1960 (2002).

[19] S. Mihardja, A. J. Spakowitz, Y. Zhang, and C. Bustamante, Proc. Natl. Acad. Sci. USA **103**, 15871 (2006).

[20] F. Wang and D. P. Landau, Phys. Rev. Lett. **86**, 2050 (2001); C. Zhou, T. C. Schulthess, S. Torbrügge, and D. P. Landau, *ibid.* **96**, 120201 (2006).

[21] G.-M. Nam, N.-K. Lee, H. Mohrbach, A. Johner, and I. M. Kulić, Europhys. Lett. **100**, 28001 (2012).

[22] To obtain quantitative measures of the differences in DNA accessibility of open versus crossed linkers, more detailed protein-accessible surface-area calculations on linkers averaged over the 3D conformational ensemble of longer nucleosome arrays is required.

[23] R. Buning, W. Kropff, K. Martens, and J. van Noort, J. Phys.: Condens. Matter **27**, 064103 (2015).

[24] K. J. Polach and J. Widom, J. Mol. Biol. **254**, 130 (1995); **258**, 800 (1996).

[25] A. Celedon, I. M. Nodelman, B. Wildt, R. Dewan, P. Searson, D. Wirtz, G. D. Bowman, and S. X. Sun, Nano Lett. **9**, 1720 (2009).

[26] T. Schalch, S. Duda, D. F. Sargent, and T. J. Richmond, Nature (London) **436**, 138 (2005).

[27] A. Maitra and G. Arya, Phys. Rev. Lett. **104**, 108301 (2010).

[28] G. Arya and T. Schlick, Proc. Natl. Acad. Sci. USA **103**, 16236 (2006).

[29] M. G. Poirier, E. Oh, H. S. Tims, and J. Widom, Nat. Struct. Mol. Biol. **16**, 938 (2009).

[30] W. Koopmans, R. Buning, T. Schmidt, and J. van Noort, Biophys. J. **97**, 195 (2009).

[31] I. V. Dobrovolskaia and G. Arya, Biophys. J. **103**, 989 (2012).

[32] M. Kruithof and J. van Noort, Biophys. J. **96**, 3708 (2009).

[33] I. M. Kulić and H. Schiessel, Phys. Rev. Lett. **92**, 228101 (2004).

[34] B. Sudhanshu, S. Mihardja, E. F. Koslover, S. Mehraeen, C. Bustamante, and A. J. Spakowitz, Proc. Natl. Acad. Sci. USA **108**, 1885 (2011).

[35] M. Y. Sheinin, M. Li, M. Soltani, K. Luger, and M. D. Wang, Nat. Commun. **4**, 2579 (2013).

[36] C. Bécavin, M. Barbi, J.-M. Victor, and A. Lesne, Biophys. J. **98**, 824 (2010).